The Pacific's Response to Surface Heating in 130 Yr of SST: La Niña–like or El Niño–like?

KA-KIT TUNG AND JIANSONG ZHOU

Department of Applied Mathematics, University of Washington, Seattle, Washington

(Manuscript received 23 March 2010, in final form 21 April 2010)

ABSTRACT

Using a modified method of multiple linear regression on instrumented sea surface temperature (SST) in the two longest historical datasets [the Extended Reconstructed SST dataset (ERSST) and the Met Office Hadley Centre Sea Ice and SST dataset (HadISST)], it is found that the response to increased greenhouse forcing is a warm SST in the mid- to eastern Pacific Ocean in the equatorial region in the annual or seasonal mean. The warming is robustly statistically significant at the 95% confidence level. Consistent with this, the smaller radiative heating from solar forcing produces a weak warming also in this region, and the spatial pattern of the response is neither La Niña–like nor El Niño–like. It is noted that previous reports of a cold-tongue (La Niña–like) response to increased greenhouse or to solar-cycle heating were likely caused by contaminations due to the dominant mode of natural response in the equatorial Pacific. The present result has implications on whether the Walker circulation is weakened or strengthened in a warmer climate and on coupled atmosphere–ocean climate model validation.

1. Introduction

El Niño Southern Oscillation (ENSO) is a dominant mode of natural oscillation of the equatorial coupled atmosphere–ocean system in the Pacific Ocean. The question of whether the equatorial Pacific responds to radiative heating in a La Niña–like (cold ENSO) pattern or an El Niño–like (warm ENSO) pattern is under debate in the context of global warming (see Vecchi et al. 2008). It has been argued that because of the tight coupling of the atmospheric Walker circulation with the thermocline depth in the eastern equatorial Pacific Ocean, the response to a larger radiative heating may not necessarily be a warmer sea surface temperature (SST). There are currently two competing theories, differing in the degree to which the atmosphere is coupled to the ocean. Clement et al. (1996) presumed that the eastern Pacific SST is controlled by ocean cold-water upwelling, and therefore a basinwide heating increases only the SST in the western Pacific. The resulting east–west temperature gradient strengthens the atmospheric Walker circulation, whose easterly flow near the surface induces stronger ocean upwelling in the eastern Pacific, thus a cold-ENSO-like response. On the other hand, Held and Soden (2006) and Vecchi and Soden (2007) suggested that tropical circulations, especially zonal overturning circulations (such as the Walker circulation) would weaken in a warmer climate. The weakened surface easterlies lead to an El Niño (warm ENSO)–like SST, of a warm tongue in the eastern Pacific. Held and Soden (2006) pointed out that this is a robust response of the current crop of coupled atmosphere–ocean general circulation models: As the SST warms, convection actually decreases, because the lower-tropospheric water vapor increases faster than the global mean precipitation. Xie et al. (2010) suggested that the warming pattern should be less El Niño-like because of the strengthened southeasterlies south of the equator, which are due to hemispheric asymmetry in land–sea area (Liu et al. 2005). Observational evidence is ambiguous. Vecchi et al. (2008) showed that the trend in 1880–2005 has a cold-ENSO-like pattern in one dataset [The Met Office Hadley Centre Sea Ice and SST dataset (HadISST)] but a warm-ENSO-like pattern with asymmetry in another [the Extended Reconstructed SST dataset (ERSST)]. Karnauskas et al. (2009) found that the zonal SST gradient strengthened in boreal autumn but weakened in spring. We hope to reconcile these disparate results in the present study.

Corresponding author address: Ka-Kit Tung, Dept. of Applied Mathematics, Box 352420, University of Washington, Seattle, WA 98195.
E-mail: ktung@uw.edu

DOI: 10.1175/2010JAS3510.1

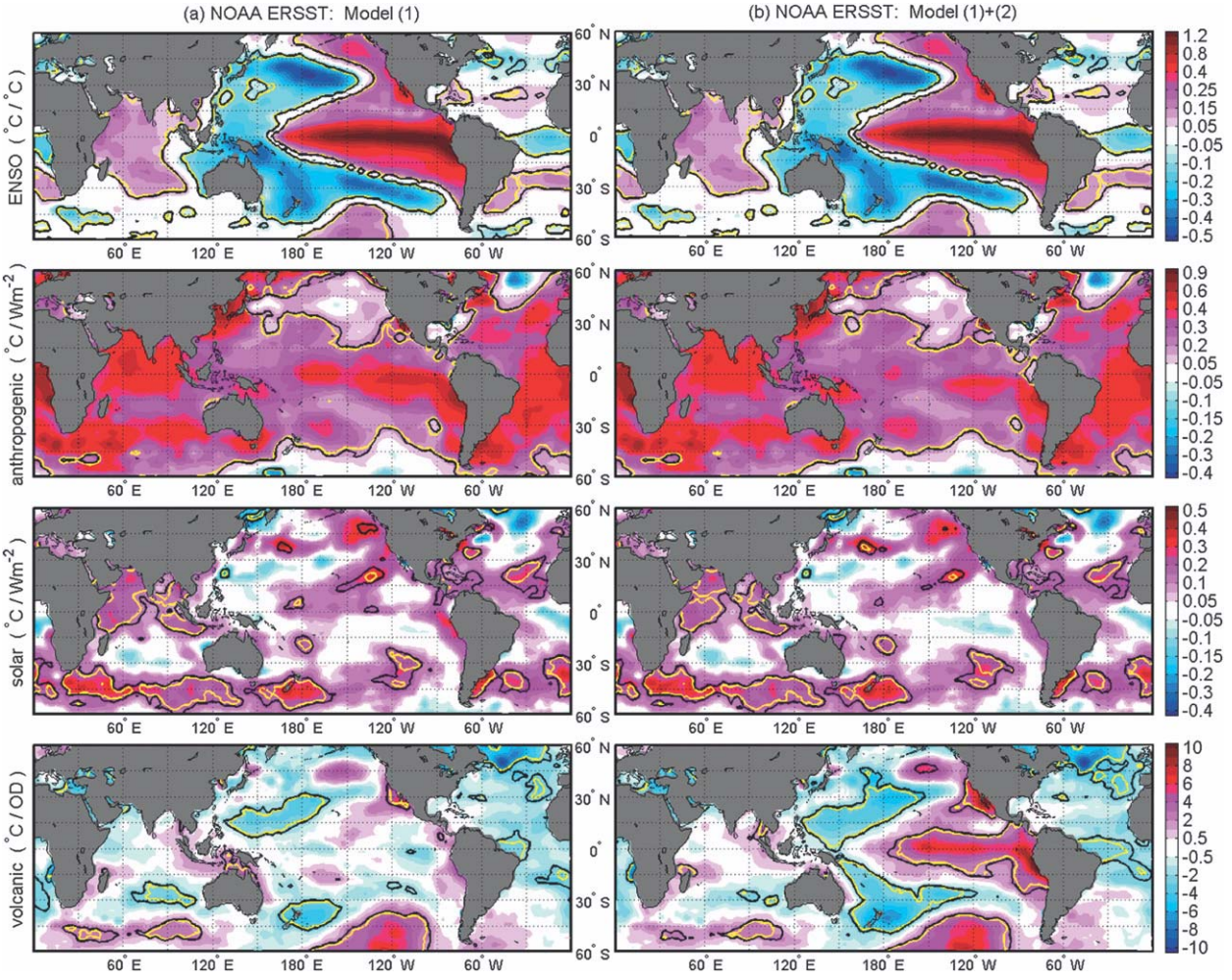

FIG. 1. Spatial pattern in annual mean SST response obtained using (a) multiple linear regression method (1) and (b) model (1) + (2) using ERSST data for responses to (top–bottom) ENSO, net anthropogenic forcing, solar forcing, and volcano aerosols. Yellow (black) contours enclose regions of 95% confidence level in a two-tailed (one-tailed) test after prewhitening. The solar response is in degrees Celsius per watt per square meter of variation in the solar constant (TSI), which in recent decades (since direct satellite measurement) varies by about 1 W m^{-2} between solar maximum and solar minimum. The anthropogenic response is in degrees Celsius per watt per square meter of net radiative forcing (RF; at the top of the troposphere). The RF change since 1880 is about 1.8 W m^{-2}. The ENSO response is in degrees Celsius per degrees Celsius of the CTI index. The aerosol response is in degrees Celsius per optical depth variation of the aerosol index.

A related phenomenon is that of the 11-yr solar cycle. Does the tropical Pacific respond with a La Niña-like or an El Niño-like pattern during solar maximum, when the solar radiation is about 0.1% stronger than during solar minimum? Because the time scales for tropical convection and for ENSO responses are much shorter than both 11 yr and the multidecadal scale of greenhouse gas increases, these mechanisms in the equatorial Pacific should be equally applicable to the two phenomena. A recent series of papers by Meehl and Arblaster (2009), Meehl et al. (2009), Van Loon and Meehl (2008), and Van Loon et al. (2007) shows that the equatorial Pacific responds in a prominent symmetric *cold*-ENSO-like pattern during the northern winter season of the peak solar year, as compared with climatology. The mechanism proposed by the authors is a variant of the ''ocean thermostat'' mechanism of Clement et al. (1996), with an additional detail of positive cloud feedback: A basinwide radiative heating will preferentially heat the eastern Pacific, which is more cloud-free because of the colder SST. The authors suggested that the increased evaporation does not locally form clouds but is instead transported by the surface easterlies to the western Pacific and that the Walker circulation is strengthened instead of weakened, keeping the eastern Pacific cloud-free. Meehl et al. (2009) proposed this as an amplifying mechanism for the

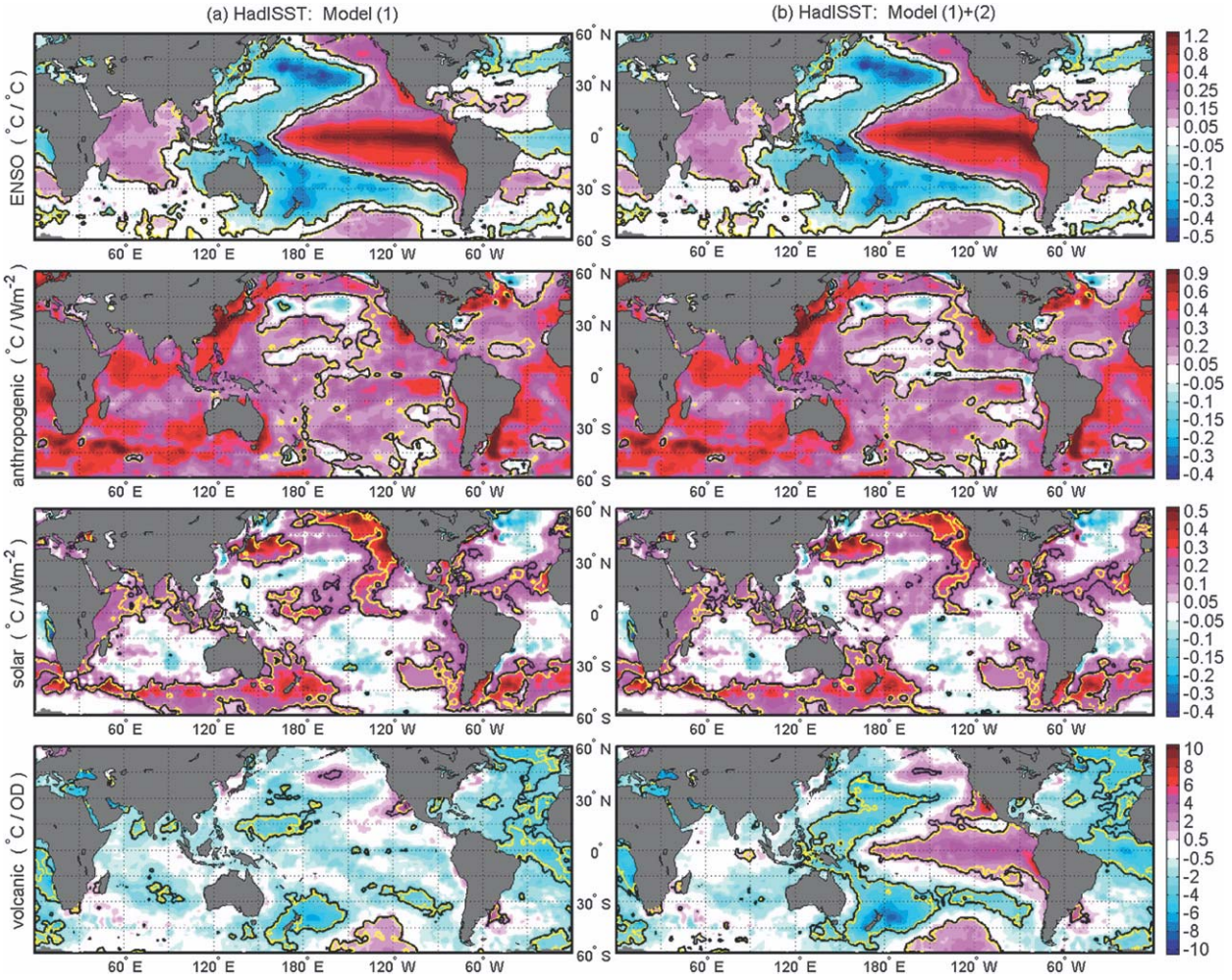

FIG. 2. As in Fig. 1, but using HadISST data.

response to solar forcing. The referenced work of Gleisner and Thejll (2003) appears to support a strengthened Walker circulation. However, Coughlin and Tung (2006) have showed that the Gleisner and Thejll results were problematic.

The van Loon–Meehl ''solar response'' pattern is *not* a response to solar forcing, because the level of total solar irradiance (TSI) for the 11 sunspot peaks used, relative to the 1968–96 ''climatology'' that was subtracted from it, is almost zero [the January–February (JF) mean difference is -0.021 W m^{-2}, as compared with a typical value of 1 W m^{-2} variation from solar maximum to solar minimum]. Our second argument is that their response, if it were solar related, would have been opposite in peak sunspot minimum years compared to the peak maximum years. Yet they did not find a warm-ENSO-like pattern in the former, while a cold-ENSO-like pattern was found in the latter. Of the 11 sunspot peak years studied by Van Loon et al. (2007), eight (1883, 1893, 1917, 1937, 1957, 1968, 1979, and 1989) are cold-ENSO years, and three (1905, 1928, and 1947) belong to warm ENSO [with the classification defined by the cold-tongue index (CTI) in January–February mean]. Van Loon and Meehl (2008) mentioned 1989 as the only cold event, but 1893, not mentioned, was even colder. Van Loon and Meehl (2008) later added three more solar peak years (1860, 1870, and 2000) to the time series, all of them belonging to cold ENSO. It is therefore not surprising that their ''solar peak'' patterns take the beautiful form of a La Niña pattern. In the solar-minimum peak years, distribution of warm- and cold-ENSO years is even, and hence no coherent pattern was found [see the previous argument of Roy and Haigh (2010)].

A common technique for disentangling responses to multiple phenomena is the method of multiple linear regression. A modified version is employed next.

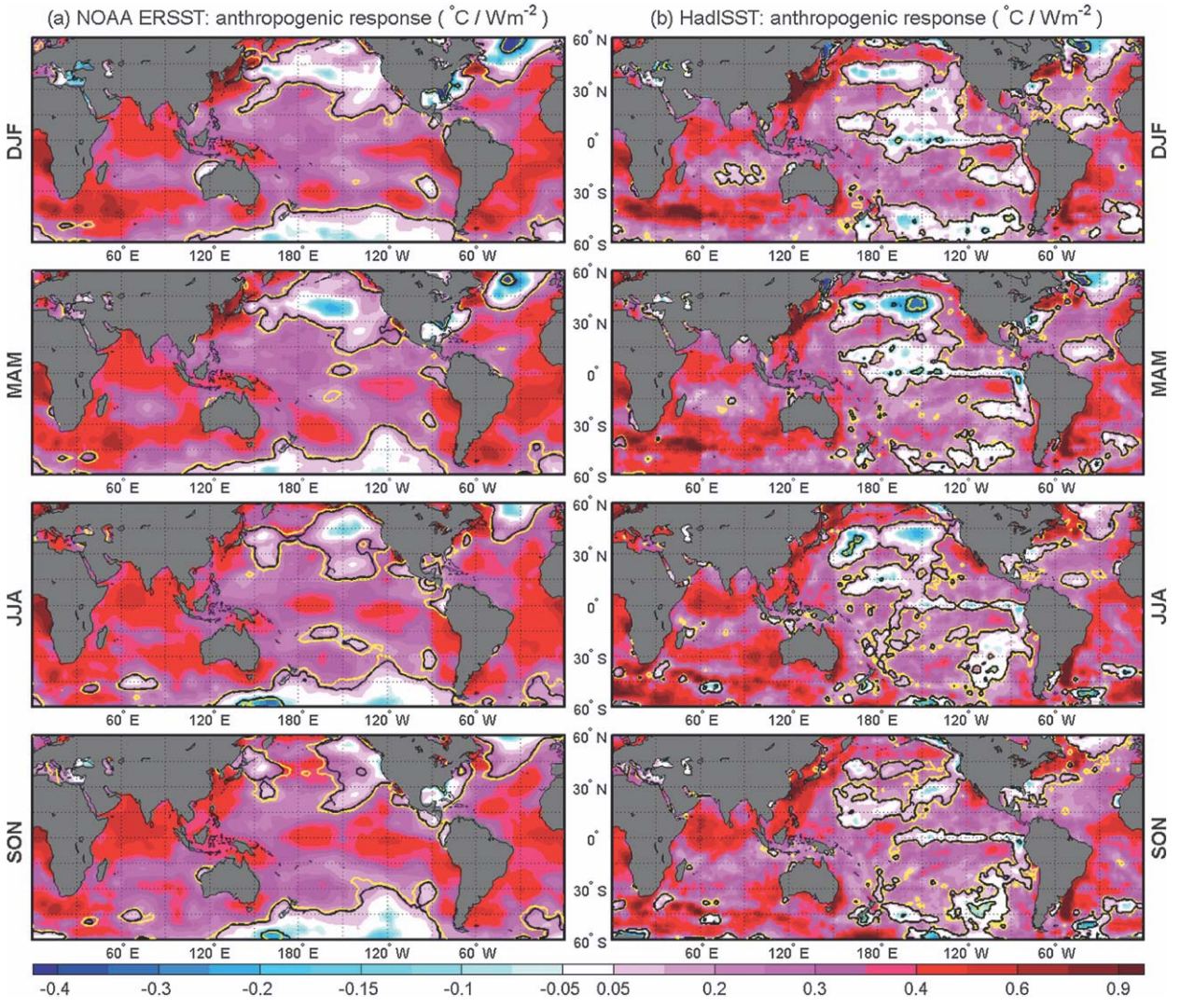

FIG. 3. Seasonal anthropogenic responses from model (1) + (2), using (a) ERSST data and (b) HadISST data for 1882–2008. Monthly data for SST and the indices were used in the multiple regression, except that G was only available as annual means. Monthly data are not available before 1882 for the TSI.

2. Multiple linear regression

We use the instrumented record of surface temperature from 1880 to 2008, in the form of the ERSST (NOAA_ERSST_V3 data, provided by the National Oceanic and Atmospheric Administration/Office of Oceanic and Atmospheric Research/Earth System Research Laboratory Physical Sciences Division and available online at http://www.cdc.noaa.gov/), as described in Smith and Reynolds (2003, 2004) and Smith et al. (2008). We also use the Hadley Center's Global Ocean Surface Temperature dataset, which is part of the HadISST (Rayner et al. 2003) and is available from 1870 to the present (available online at http://hadobs.metoffice.com/hadisst/).

In the multiple regression study, it is assumed that the SST variation in space $\mathbf{x}$ (a vector) and time t can be modeled by

$$\mathrm{SST}(\mathbf{x}, t) = p_S(\mathbf{x})\mathrm{TSI}(t) + p_E(\mathbf{x})\mathrm{CTI}(t) + p_G(\mathbf{x})G(t) + p_V(\mathbf{x})V(t) + \varepsilon(\mathbf{x}, t), \quad (1)$$

where G is the anthropogenic greenhouse emissions (Hansen et al. 2007) (text file available online at http://data.giss.nasa.gov/modelforce/), V is the volcano aerosol index (Sato et al. 1993), and ε is the remainder and may or may not be Gaussian noise. TSI is from Lean et al. (2005) and Wang et al. (2005), extended to 2008 and kindly provided to us by J. Lean (2010, personal communication). CTI is the averaged SST over 6°N–6°S,

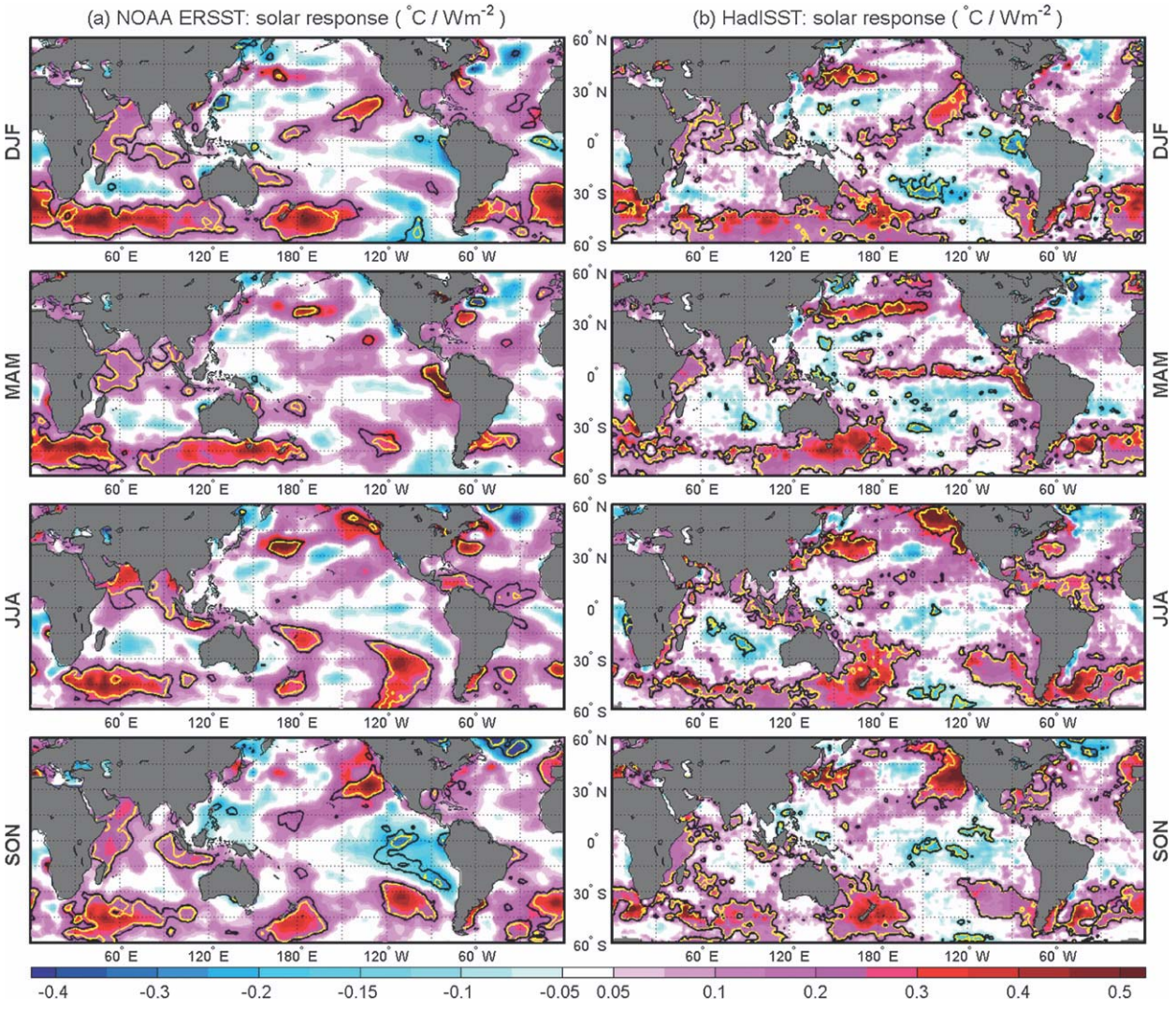

FIG. 4. As in Fig. 3, but for the solar response.

180°–90°W minus the global mean SST (offered online by the University of Washington at http://jisao.washington.edu/data/cti/).

To take into account the possibility that CTI itself could be forced by TSI, G, and V, (1) is supplemented by

$$\mathrm{CTI}(t) = \beta_S \mathrm{TSI}(t) + \beta_G G(t) + \beta_V V(t) + R(t). \quad (2)$$

The residual R obtained from (2) represents the unforced ENSO index. The nested model (1) + (2) is equivalent to model (1) alone, with the regressor CTI replaced by R. No lag is used here in the response relative to the forcing index, although Lean and Rind (2008) incorporated various lags in their multiple regression. The spatial patterns are little changed when we repeated the calculation with their lags.

Figure 1 (Fig. 2) shows the various responses p for the ERSST (HadISST) data. Figs. 1a and 2a show the result of model (1) using CTI as the ENSO index, and Figs. 1b and 2b use the unforced ENSO index R. A two-tailed Student's t test (yellow contour) answers the question of whether the signal is different from zero, while the one-tailed t test (black contour) tests whether the signal is positive or negative. Some of the previous applications of Student's t tests may have overestimated the statistical significance by assuming ε to be white noise, while it is positively autocorrelated in reality (see Fig. A1). Here the t test is applied only over the locations that pass the Durbin–Watson test. In other regions, additional processing to take autocorrelation into account is required (see the appendix).

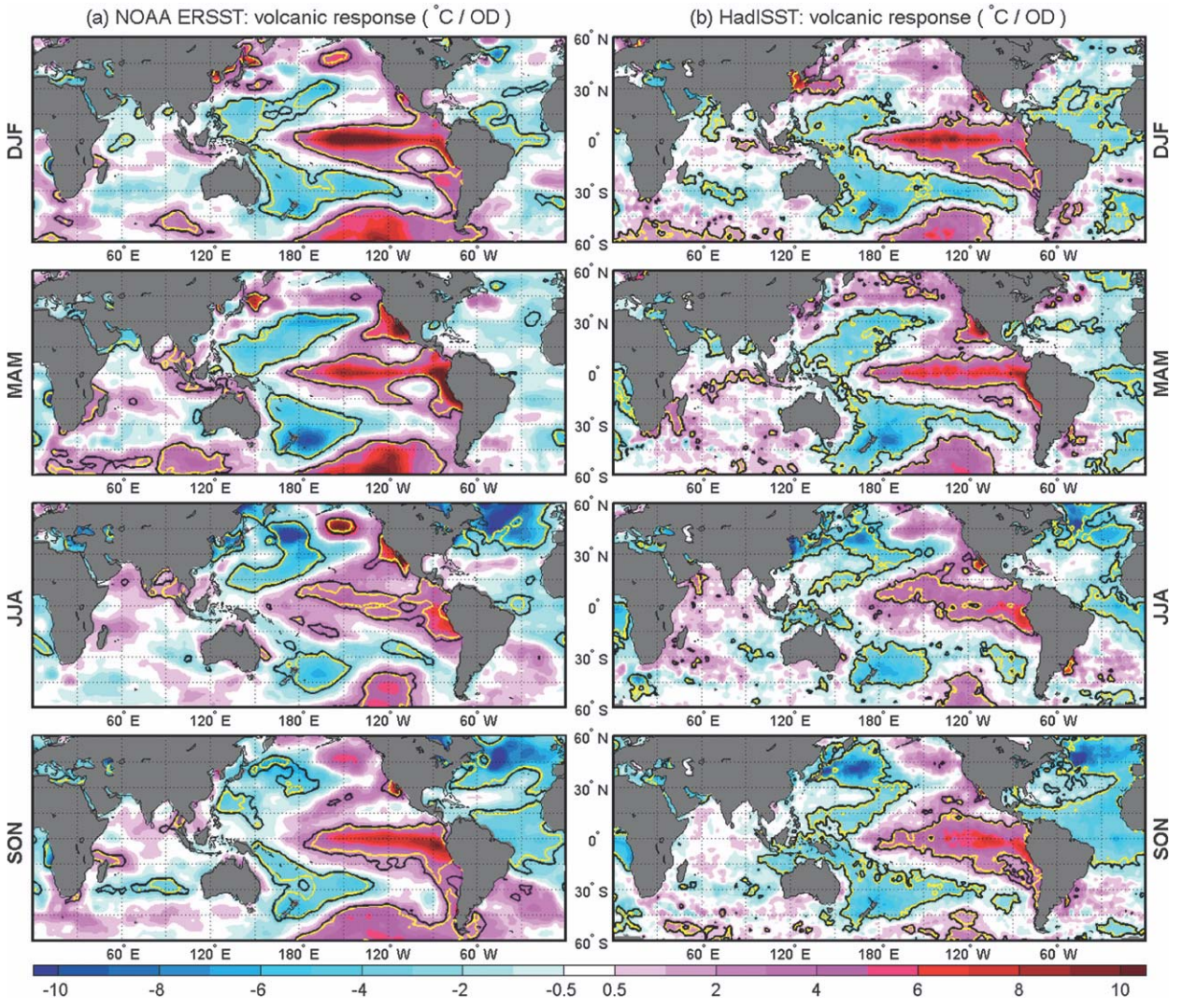

FIG. 5. As in Fig. 3, but for the volcano response.

a. *Anthropogenic response*

Anthropogenic response is warming in almost the entire Pacific, and the signal is statistically significant above the 95% confidence level. There is very little projection of G onto CTI, and so there is not much difference between the left and right panels of either Fig. 1 or Fig. 2. The anthropogenic warming is consistent with the sea level pressure result of Vecchi et al. (2006) that showed a weakening of the Walker circulation. The results for the two datasets are consistent. There is, however, a very thin strip over the equator in HadISST where the small anthropogenic response is not statistically significant. Such a narrow strip of different behavior likely indicates a data-quality problem. Our statistical test also shows a larger area of insignificance in the mid-Pacific in HadISST than in the ERSST case. Seasonal behavior for the anthropogenic response is shown in Fig. 3 for the two datasets using model (1) + (2), and it is consistent with the annual mean result. The contrasting behavior between the autumn and spring seasons mentioned by Karnauskas et al. (2009) is not seen in our analysis. There is again a thin strip of possibly bad data (not statistically significant) in the HadISST along the equator, which is more confined to the mid- and eastern Pacific during boreal autumn, and this may have contributed to the strengthened zonal temperature gradient in Karnauskas et al. (2009).

b. *Solar response*

Solar response is weakly warm in the equatorial Pacific, as was previously found by Roy and Haigh (2010) using a multiple regression model similar to our model (1) and by

Zhou and Tung (2010) using a different method. This warming is not statistically significant, in annual mean or in seasonal mean, when we use model (1) + (2) (Fig. 4). It is neither El Niño–like nor La Niña–like. It looks nothing like the large (~−1°C) cold tongue found by Van Loon et al. (2007). This does not mean that there is no solar response; it just means that the amplitude of the response in the equatorial Pacific is too weak. Zhou and Tung (2010) established that the global SST pattern is related to solar forcing.

c. *Volcano response*

Volcanic aerosol forcing projects partly onto the CTI. While the response obtained using CTI as the regressor is weakly negative in the Pacific, it becomes warm-ENSO-like when R is used as the regressor (Fig. 5). The result is statistically significant and appears consistent with the earlier suggestion of Handler (1984). However, there is uncertainty in the choice of the volcano index, and the time behavior of the response a few years after the eruption may not follow the aerosol optical depth.

We repeated the calculation without using V as one of the regressors, and our previous responses to anthropogenic, solar, and ENSO indices are little changed; so, these responses are unaffected by the choice of volcano index.

3. Conclusions

We have demonstrated that in the tropical Pacific the anthropogenic or solar forcing produces mostly a warmer sea surface temperature, but the spatial pattern is not in the form of an ENSO-like warm tongue or cold tongue. There is consistency in such responses in two different sea surface temperature datasets of long duration. The warming response in the tropical Pacific to greenhouse forcing is consistent with recent Intergovernmental Panel on Climate Change model results (Vecchi et al. 2008; Xie et al. 2010). The magnitude of solar warming is found in this region to be about 0.1° ± 0.3°C. The much larger response (of 1°C cooling in a beautiful cold tongue in the equatorial Pacific) found by Van Loon and Meehl (2008) is likely due to ENSO and not to the amplifying effect of positive cloud feedback.

Acknowledgments. The research is supported by National Science Foundation, Climate Dynamics Program, under Grant ATM 0808375. We thank Dr. Gabriel Vecchi and two anonymous reviewers for their helpful comments.

APPENDIX

Student's *t* Tests and Prewhitening

The multiple linear regression model takes the form

$$\mathbf{Y}(t) = \sum_{j=1}^{k} \mathbf{x}_j(t)\beta_j + \varepsilon(t),$$

where the regressors $\mathbf{x}_j(t)$ are predetermined and the error $\varepsilon(t)$ is unobserved. Given n observations $\{Y_i, x_{i1}, \ldots, x_{ik}\}_{i=1}^{n}$, the ordinary least squares (OLS) fitting gives the estimators $\hat{\beta}_j$ of the unknown regression coefficients β_j in vector form as $\boldsymbol{\beta} = M\mathbf{Y}$, where $M = (\mathbf{X}^{\mathrm{T}}\mathbf{X})^{-1}\mathbf{X}^{\mathrm{T}}$ and $\mathbf{X}$ is an $n \times k$ matrix of observations of all the regressors. If the error is independent and identically distributed normal: $N(0, \sigma^2)$, then the Gaussian distribution of

$$\hat{\beta}_j \sim N\left(\beta_j, \sum_{i=1}^{n} M_{ji}^2\sigma^2\right)$$

follows. Furthermore, it can be shown that $\mathrm{RSS}/\sigma^2 \sim \chi_{n-k}^2$, where

$$\mathrm{RSS} = \sum_{i=1}^{n}\left(Y_i - \sum_{j=1}^{k} x_{ij}\hat{\beta}_j\right)^2$$

is the residual sum of squares, and $S^2 = \mathrm{RSS}/(n-k)$ is independent of any $\hat{\beta}_j$. Therefore

$$(\hat{\beta}_j - \beta_j)\Big/\sqrt{S^2\sum_{i=1}^{n} M_{ji}^2} \sim t_{n-k}$$

for $j = 1, \ldots, k$. This expression can be used to form a Student's t test of the null hypothesis H_0: $\beta_j = 0$ versus the alternative hypothesis H_1: $\beta_j \neq 0$ (two sided) or H_1: $\beta_j > 0$ (one sided; H_1: $\beta_j < 0$ is tested in a similar way). We reject H_0 at significance level α in favor of H_1: $\beta_j \neq 0$ if

$$\left|(\hat{\beta}_j - 0)\Big/\sqrt{S^2\sum_{i=1}^{n} M_{ji}^2}\right| > t_{n-k,\alpha/2}$$

and in favor of $\beta_j > 0$ if

$$(\hat{\beta}_j - 0)\Big/\sqrt{S^2\sum_{i=1}^{n} M_{ji}^2} > t_{n-k,\alpha}.$$

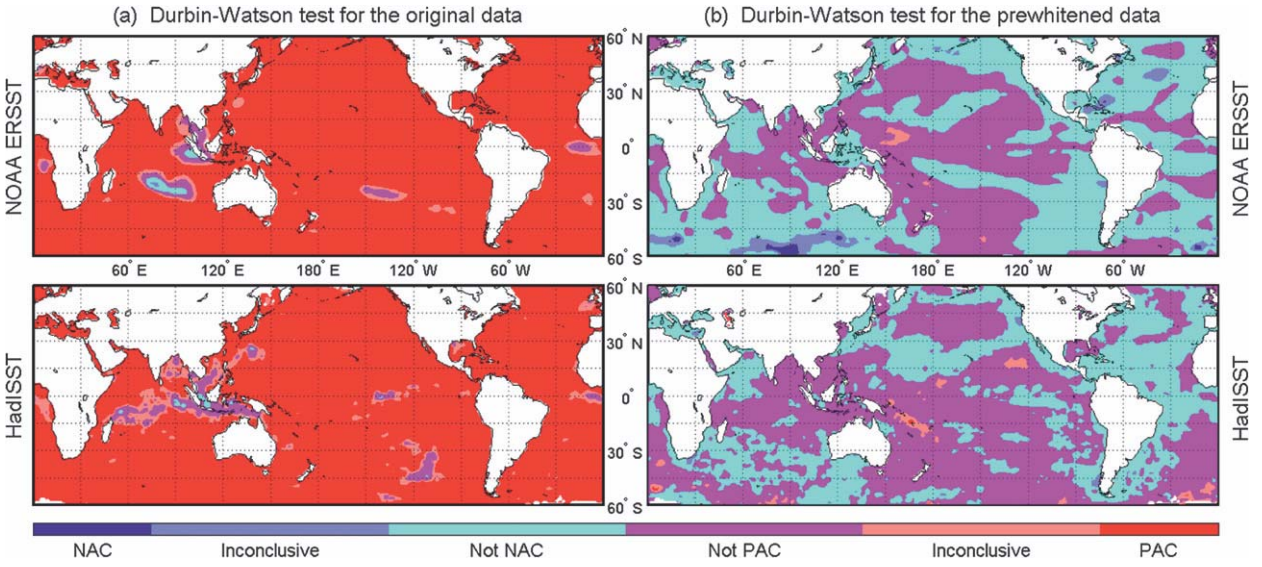

FIG. A1. Durbin–Watson test on the residual (a) in the original data, which are shown to be positively autocorrelated (PAC), and (b) after one stage of prewhitening, which then become neither positively autocorrelated nor negatively autocorrelated (NAC), for (top) ERSST data and (bottom) HadISST data.

In climate data the errors are usually autocorrelated, and so the above analysis does not apply directly. The Durbin–Watson test (Durbin and Watson 1971; Savin and White 1977) can be used to detect the presence of autocorrelation in the residuals from a regression analysis. In the case of autocorrelated error terms [suppose they are AR(1): $\varepsilon(t+1) = \rho\varepsilon(t) + \omega(t+1)$], a two-stage regression can be employed to correct the model as follows: 1) Fit a linear model to the original data by OLS. 2) Estimate the autocorrelation ρ with the sample value

$$\hat{\rho} = \sum_{t=2}^{n} (\hat{\varepsilon}_t \hat{\varepsilon}_{t-1}) \Big/ \sum_{t=1}^{n} \hat{\varepsilon}_t^2,$$

where $\hat{\varepsilon}_t$ is the residual from the first step analysis. 3) Prewhiten the data using $\hat{\rho}$ and then refit the model. The prewhitening process is done by introducing new data $\tilde{Y}_{i+1} = Y_{i+1} - \hat{\rho}Y_i$ and regressors $\tilde{x}_{i+1,j} = x_{i+1,j} - \hat{\rho}x_{ij}$ for $i = 1, \ldots, n-1$ and $j = 1, \ldots, k$. Now the model becomes

$$\tilde{Y}(t+1) = \sum_{j=1}^{k} \tilde{x}_j(t+1)\beta_j + \tilde{\varepsilon}(t+1)$$

with the new noise $\tilde{\varepsilon}(t+1) = \omega(t+1) + (\rho - \hat{\rho})\varepsilon(t)$. The Durbin–Watson test can be applied to the new noise. If it does not satisfy the test, the prewhitening process is repeated. This has not been necessary in our case (see Fig. A1). Last, the statistical significance of regression coefficients obtained from a model with white noise can be tested as above using the Student's t test.

REFERENCES

Clement, A. C., R. Seager, M. A. Cane, and S. E. Zebiak, 1996: An ocean dynamical thermostat. *J. Climate,* **9,** 2190–2196.

Coughlin, K., and K. K. Tung, 2006: Misleading patterns in correlation maps. *J. Geophys. Res.,* **111,** D24102, doi:10.1029/2006JD007452.

Durbin, J., and G. S. Watson, 1971: Testing for serial correlation in least squares regression, III. *Biometrika,* **58,** 1–19.

Gleisner, H., and P. Thejll, 2003: Patterns of tropospheric response to solar variability. *Geophys. Res. Lett.,* **30,** 1711, doi:10.1029/2003GL017129.

Handler, P., 1984: Possible association of stratospheric aerosols and El Niño type events. *Geophys. Res. Lett.,* **11,** 1121–1124.

Hansen, J., and Coauthors, 2007: Climate simulations for 1880–2003 with GISS modelE. *Climate Dyn.,* **29,** 661–696.

Held, I. M., and B. J. Soden, 2006: Robust responses of the hydrological cycle to global warming. *J. Climate,* **19,** 5686–5699.

Karnauskas, K. B., R. Seager, A. Kaplan, Y. Kushnir, and M. A. Cane, 2009: Observed strengthening of the zonal sea surface temperature gradient across the equatorial Pacific Ocean. *J. Climate,* **22,** 4316–4321.

Lean, J., and D. Rind, 2008: How natural and anthropogenic influences alter global and regional surface temperatures: 1889 to 2006. *Geophys. Res. Lett.,* **35,** L18701, doi:10.1029/2008GL034864.

——, G. J. Rottman, J. Harder, and G. Kopp, 2005: SORCE contributions to new understanding of global change and solar variability. *Sol. Phys.,* **230,** 27–53.

Liu, Z., S. Vavrus, F. He, N. Wen, and Y. Zhong, 2005: Rethinking tropical mean response to global warming. *J. Climate,* **18,** 4684–4700.

Meehl, G. A., and J. M. Arblaster, 2009: A lagged warm event-like response to peaks in solar forcing in the Pacific region. *J. Climate,* **22,** 3647–3660.

——, ——, K. Matthes, F. Sassi, and H. Van Loon, 2009: Amplifying the Pacific climate system response to a small 11-year solar cycle forcing. *Science,* **325,** 1114–1118.

Rayner, N. A., D. E. Parker, E. B. Norton, C. K. Folland, L. V. Alaxander, D. P. Rowell, E. C. Kent, and A. Kaplan, 2003: Global analyses of sea surface temperature, sea ice, and night marine air temperature since the late nineteenth century. *J. Geophys. Res.,* **108,** 4407, doi:10.1029/2002JD002670.

Roy, I., and J. Haigh, 2010: Solar cycle signals in sea level pressure and sea surface temperature. *Atmos. Chem. Phys.,* **10,** 3147–3153.

Sato, K., J. E. Hansen, M. P. McCormick, and J. B. Pollack, 1993: Stratospheric aerosol optical depths, 1850–1990. *J. Geophys. Res.,* **98,** 22 987–22 994.

Savin, N. E., and K. J. White, 1977: The Durbin–Watson test for serial correlation with extreme sample sizes or many regressors. *Economitrica,* **45,** 1989–1996.

Smith, T. M., and R. W. Reynolds, 2003: Extended reconstruction of global sea surface temperatures based on COADS data (1854–1997). *J. Climate,* **16,** 1495–1510.

——, and ——, 2004: Improved extended reconstruction of SST (1854–1997). *J. Climate,* **17,** 2466–2477.

——, ——, T. C. Peterson, and J. Lawrimore, 2008: Improvements to NOAA's historical Merged Land–Ocean Surface Temperature Analysis (1880–2006). *J. Climate,* **21,** 2283–2296.

Van Loon, H., and G. A. Meehl, 2008: The response in the Pacific to the sun's decadal peaks and contrasts to cold events in the Southern Oscillation. *J. Atmos. Sol. Terr. Phys.,* **70,** 1046–1055.

——, ——, and D. J. Shea, 2007: Coupled air–sea response to solar forcing in the Pacific region during northern winter. *J. Geophys. Res.,* **112,** D02108, doi:10.1029/2006JD007378.

Vecchi, G. A., and B. J. Soden, 2007: Global warming and the weakening of tropical circulation. *J. Climate,* **20,** 4316–4340.

——, ——, A. T. Wittenberg, and I. M. Held, 2006: Weakening of tropical Pacific atmospheric circulation due to anthropogenic forcing. *Nature,* **441,** 73–76.

——, A. Clement, and B. J. Soden, 2008: Examining the tropical Pacific's response to global warming. *Eos, Trans. Amer. Geophys. Union,* **89,** 81–83.

Wang, Y.-M., J. Lean, and N. R. Sheeley Jr., 2005: Modeling the sun's magnetic field and irradiance since 1713. *Astrophys. J.,* **625,** 522–538.

Xie, S.-P., C. Deser, G. A. Vecchi, J. Ma, H. Teng, and A. T. Wittenberg, 2010: Global warming pattern formation: Sea surface temperature and rainfall. *J. Climate,* **23,** 966–986.

Zhou, J., and K. K. Tung, 2010: Solar cycle in 150 years of global sea surface temperature data. *J. Climate,* **23,** 3234–3248.